Folded Microstrip Resonator

Bal S.Virdee, Christos Grassopoulos†

London Metropolitan University, Dept. of Computing, Communications Technology & Mathematics, 166-220 Holloway Road, London N7 8DB, U.K., Email: b.virdee@londonmet.ac.uk
†Astrium Ltd, Gunnels Wood Road, Stevenage, Hertfordshire, SG1 2AS, U.K., Email: christos.grassopoulos@astrium-space.com

Abstract **A compact concertina shaped microstrip ring resonator, referred to here as a 'folded ring' resonator is shown to behave analogously to a microstrip annular-ring resonator. The folded ring resonator resonates at identical resonant mode frequencies as the annular-ring resonator, which is designed to operate at the same fundamental mode frequency and when fabricated on an identical dielectric substrate. It is also demonstrated that the folded ring when cut in half, referred to here as a 'folded half-ring' resonator, also exhibits similar transmission characteristics to a conventional annular-ring resonator. This resonator structure is even more compact. In addition, an input/output-coupling scheme to the resonator is employed that significantly improves the insertion loss and return loss performance of the resonant structures.**

I. Introduction

The traditional use of microstrip ring resonator is for characterising microstrip parameters such as effective dielectric constant, discontinuity, phase velocity and dispersion of transmission lines [1]. Its geometrical simplicity, moderate Q-factor and low radiation loss properties has made it an attractive candidate for a variety of applications such as oscillators, tuned amplifiers, filters, mixers, and antennas [2]-[5], where a compact structure is more preferable than highest possible Q-factor. However, its large physical size can present a drawback, especially for designs at low microwave frequencies. In this paper, a folded ring and folded half-ring resonant structures are shown to have analogous transmission characteristics to a conventional annular-ring microstrip resonator with the advantage of being significantly more compact.

II. Folded Ring and Folded Half-Ring Resonators

The folded ring structure comprises of a regular ring that has been folded into a concertina shape, which includes of symmetrically located input/output microstrip feed lines, coupling gaps to allow the propagation of electromagnetic energy at its resonant frequencies. It is important that curved bends are used to form the folded resonators in order to prevent unnecessary excitation of undesired degenerate modes other then the regular ring modes. The folded ring shows the resonant transmission peaks at frequencies f_n given by [5]

$$f_n = \frac{nc}{2\pi r\sqrt{\varepsilon_{eff}}} \text{ or } 2\pi r = n\lambda_g \quad (1)$$

where n is a positive integer, c the speed of light in a vacuum, r is the mean radius, ε_{eff} the effective dielectric constant, and λ_g the guided wavelength.

The folded half-ring resonator comprises of the folded ring structure that is cut into one half. The coupling is implemented at the maximum electric-field points located at the open-ends of the resonators. The length of the folded half-ring corresponds to half the circumference length of the regular ring resonator. Since the regular ring is composed of two half-wavelength linear resonators, which are connected in parallel, the theoretical analysis of the regular ring resonator can be applied to the folded half-ring structure. This means that the folded half-ring structure supports waves that have an integral multiple of half-guided wavelength ($n\lambda_g/2$) equal to its mean length (πr), expressed by Equation (1).

Figure 1 illustrates the relative dimensions of conventional ring, the folded ring, the folded half-ring and a half-wavelength resonator, which are designed to resonate at a fundamental mode (n=1) of 3 GHz. The length of the 50 Ω half-wavelength resonator is 36.68 mm, the diameter of the ring is 24.4 mm, and the folded ring occupies a space of 10.50 mm x 13.55 mm. The conventional ring, folded ring, and folded half-ring have a width (w) of 0.5 mm, which corresponds to impedance of 112.31Ω, on a substrate with a relative dielectric constant (ε_r) of 2.17 and a thickness (h) of 0.794 mm.

The length of the folded ring is consistent with the length of the circumference of a conventional ring designed to resonate at a fundamental mode (n=1) of 3 GHz. The length of the folded half-ring is one half the length of a folded ring but compensated for the open-end fringing effect. The equivalent end-effect length is calculated using [6]

$$l_{eo} = 0.412h\left(\frac{\varepsilon_{eff}+0.3}{\varepsilon_{eff}-0.258}\right)\left(\frac{w/h+0.262}{w/h+0.813}\right) \quad (2)$$

0-7803-7695-1/03/$17.00 © 2003 IEEE

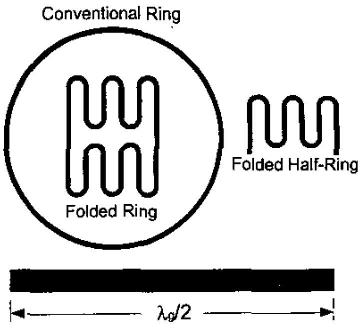

Figure 1. A comparison of the folded ring and folded half-ring resonators with the conventional ring and half-wavelength resonator designed to operate at 3 GHz.

The input/output coupling mechanism employed consists of a quarter-guide wavelength tapered section of microstrip line, which transforms the input/output impedance of 50Ω to impedance corresponding to the width of the ring. Coupling between the folded ring and the input/output is enhanced by employing edge coupling along its flat sides, which is provided by the open-circuit stubs, of length *a*, attached at the end of the input/output feed-lines next to the resonator as illustrated in Figure 2. The gap between the resonator and the input/output transmission line also govern the amount of energy coupled to the resonator. The respective input/output coupling gap, *g*, is identical, as well as the length of the coupling stubs, *a*, to preserve the symmetry of the resonator.

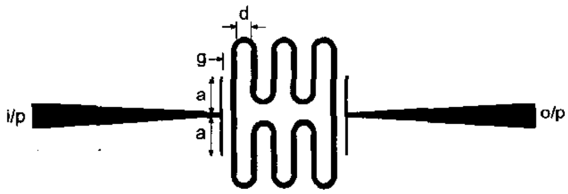

Figure 2. A folded ring resonator with tapered input/output feed-lines and enhanced coupling scheme.

The loaded Q-factor of the half-ring can be calculated using:

$$Q = {}^{\omega_o}\!/_{\Delta\omega} \qquad (3)$$

Where ω_o is the resonant frequency, and $\Delta\omega$ is the 3dB bandwidth.

The microstrip resonator structures were fabricated on PTFE substrate by etching one of the copper plates with a conventional photolithographical method. Reflection and transmission spectra were measured with a HP 8510C network analyzer.

III. Simulation and Measured Results

Figures 3 to 6 depict the simulated and measured spectra of transmitted (S_{21}) and reflected (S_{11}) at the folded ring and folded half-ring resonators across a frequency range encompassing the first three resonant modes. The simulation was performed using Agilent Technologies Momentum RF, which is a 2.5D electromagnetic full wave solver based on the method of moments.

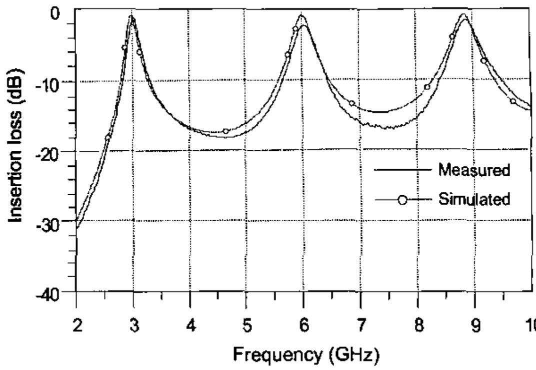

Figure 3. Simulated and measured transmission response of the folded ring resonator.

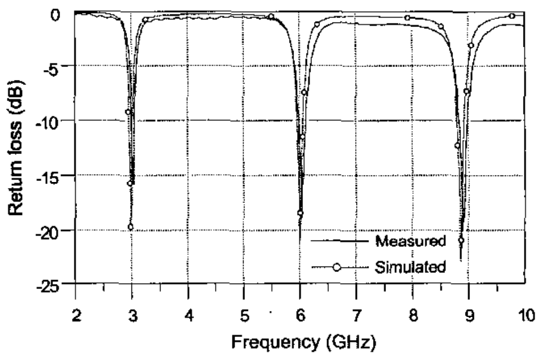

Figure 4. Simulated and measured reflection response of the folded ring resonator.

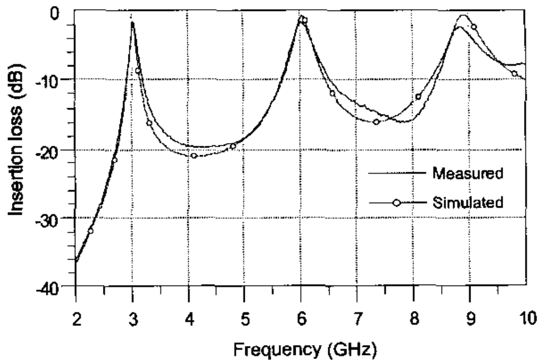

Figure 5. Simulated and measured transmission response of the folded half-ring resonator

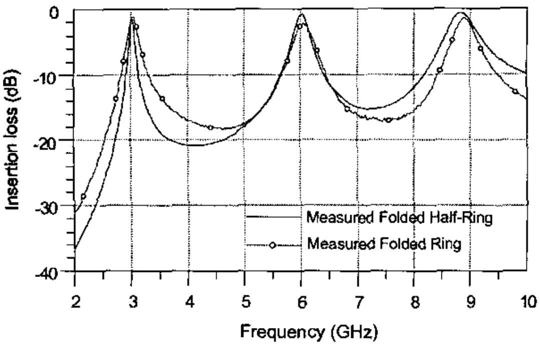

Figure 6. Comparison of the measured transmission response of the folded ring and folded half-ring resonators.

The predicted and measured resonant frequencies at the first three resonant modes are tabulated in Table 1. For the folded ring the worst case error between the measured and predicted resonant frequencies is 0.45 % at the third resonant mode. In the case of the folded half-ring the worst case error in resonant frequency is 0.64 % at $n = 3$. This discrepancy indicates how critical the shape of the folded structure is in determining higher order mode frequencies. Coupling in adjacent folds in the resonator limits the degree of compression in order to avoid excitation of degenerate modes. Table 2 shows the predicted insertion and return loss results. Table 3 shows the measured insertion and return loss results. The measurements indicate that insertion loss less than -3 dB and return loss better than -15 dB is achieved at the first three resonant modes for both the folded ring and folded half-ring resonators.

Table 1

	Simulated		*Measured*	
n	*Folded ring* f_o (GHz)	*Folded half-ring* f_o (GHz)	*Folded ring* f_o (GHz)	*Folded half-ring* f_o (GHz)
1	3.00	3.00	3.02	3.04
2	6.00	6.04	6.04	6.04
3	8.86	8.92	8.90	8.86

Table 2

	Simulated			
n	*Folded ring* *IL* (dB)	*Folded half-ring* *IL* (dB)	*Folded ring* *RL* (dB)	*Folded half-ring* *RL* (dB)
1	-0.87	-1.60	-19.72	-15.03
2	-0.79	-0.82	-21.36	-21.12
3	-0.73	-0.62	-23.15	-25.60

Table 3

	Measured			
n	*Folded ring* *IL* (dB)	*Folded half-ring* *IL* (dB)	*Folded ring* *RL* (dB)	*Folded half-ring* *RL* (dB)
1	-1.28	-1.62	-15.90	-15.91
2	-2.28	-1.70	-16.12	-16.45
3	-1.51	-2.32	-20.10	-18.53

The effect on the fundamental resonant mode, insertion loss, return loss, loaded Q-factor, and 3 dB bandwidth by varying coupling stub length, a, is shown in Figure 7. The results show that coupling stub length has relatively very little influence on the resonant mode frequency, the maximum variation obtained is 83 MHz with a length change of between 1mm to 4.5 mm. The stub length also has negligible effect on the insertion loss, however it improves the return loss quite significantly as it is increased. Return loss of -25 dB is obtained with a length of 4.5 mm. The loaded Q-factor however significantly degrades with increase in stub length. Loaded Q-factor in access of 80 can be achieved when stub length $a \leq 1$ mm. The Q-factor can also be increased at the expense of insertion loss by weakening the coupling gap in and out of the ring. The 3 dB bandwidth increases with increase in stub length. The minimum value of 3 dB bandwidth is 36 MHz at $a = 1$ mm, and the maximum is 272 MHz at $a = 4.5$ mm.

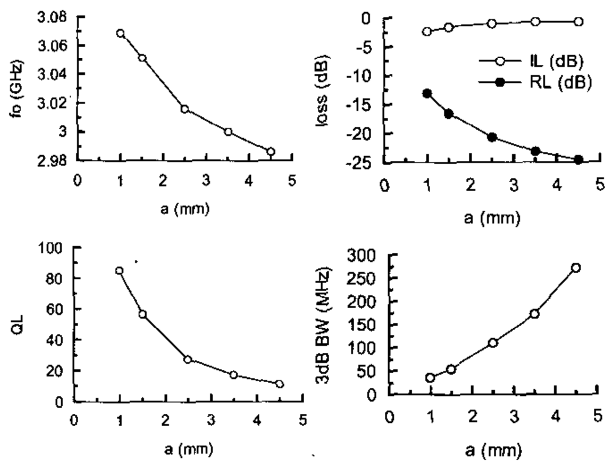

Figure 7. The effect of coupling stub length variation

Figure 8 shows the effect of squashing the folded ring, in particular decreasing the separation, d, between the adjacent folds of the ring. As d is made smaller the resonant frequency tends to increase as the coupling between the adjacent fold lines intensifies. Variation of d has negligible effect on both the insertion loss and return loss. The Q-factor abruptly increases for $d < 0.5$ mm. The maximum Q-value is ≈ 80 at $d = 0.25$ mm. The maximum insertion loss is -1.11 dB and the return loss better than -19 dB is obtained. The 3 dB bandwidth is > 280 MHz and peaks to 315 MHz at $d = 1.5$ mm.

The measured results indicate the effectiveness of the coupling scheme employed in enhancing the input/output coupling while maintaining a relative low insertion loss and a good return loss. The measurements also confirm that both the folded ring and folded half-ring resonant structures behave identically to an annular-ring resonator, where the resonant modes are a function of the annular-rings mean radius. The folded ring resonator has the advantage of occupying about one-third of the space as a conventional annular-ring resonator designed to operate at the same resonant frequency. The folded half-ring resonator is even more compact and occupies less than one-sixth of the space as a conventional annular-ring resonator. The results also show a remarkable agreement between the prediction and measurement in terms of the resonant frequency at the various resonant modes.

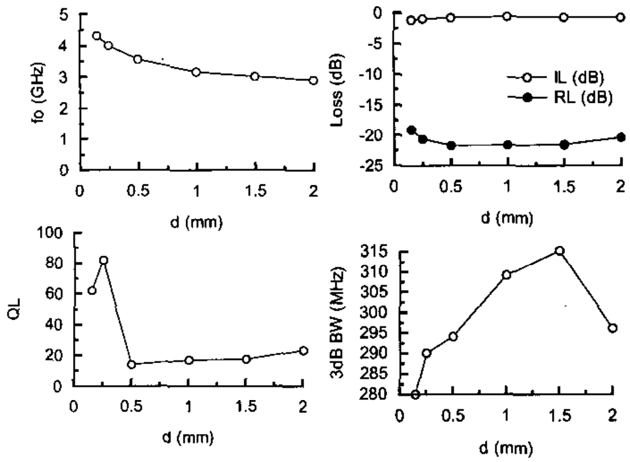

Figure 8. The effect of compressing the folded ring resonator.

IV. Folded Ring Filter Application

The two flat sides of the folded ring resonator presents an effective coupling area with input/output feed-lines, as well as with other resonators especially for designing miniature narrow or medium bandwidth band-pass filters. This kind of filter is increasingly in demand for of mobile communications systems. A typical narrow-band filter is constructed using parallel-coupled half-wavelength resonators. However, at DECT, GSM1800, UMTS bands, the physical length of parallel-coupled filters are too prohibitively long, even when fabricated on a higher dielectric constant substrate.

A two-pole folded ring filter was designed at a centre frequency of 3 GHz using a substrate having a dielectric constant ε_r = 2.17 and a thickness h = 0.794 mm. The separation between the adjacent resonators is 0.6 mm, and input/output coupling gap is 0.15 mm. The insertion loss and return loss response of the filter is shown in Figure 9.

V. Conclusions

A folded ring resonator and a folded half-ring resonator has been practically demonstrated to generate identical transmission resonant peaks as a conventional annular-ring microstrip resonator designed to operate at the same frequency and when fabricated on the same dielectric substrate. The folded ring and folded half-ring resonators significantly save space and can be employed to design filters. Compared to a conventional ring resonator that uses strong coupling, folded resonators employing the coupling scheme described above achieves a relatively low insertion loss and good return loss characteristics.

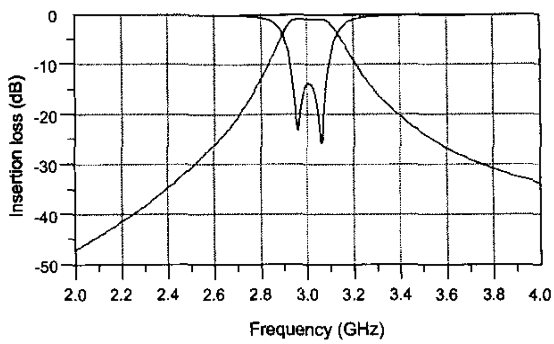

Figure 9. Transmission and reflection response of a 2-pole folded ring resonator.

Acknowledgement

The authors should like to thank Astrium Ltd. for supporting this work, and to Mr Peter Pettit at London Metropolitan University for fabricating the circuits.

References

[1] EDWARDS, T.C.: *Foundation for microstrip circuit design. New York:* Wiley, 1981.

[2] ZHU, L., and WU, K.: '*A joint field/circuit model of line-to-ring coupling structures and its application to the design of microstrip dual-mode filters and ring resonator circuits,*' IEEE Trans. Microwave Theory Tech., 1999, MTT-47, (10). pp. 1938-1948

[3] YABUKI, H., SAGAWA, M., MATSUO, M., and MAKIMOTO, M.: *'Stripline dual-mode ring resonators and their application to microwave devices,'* IEEE Trans. Microwave Theory Tech., 1996, MTT-44, (5), pp. 723-728

[4] CHANG, K., MARTIN, S. WANG, F., and KLEIN, J.L.: *'On the study of microstrip ring and varactor-tuned ring circuits,'* IEEE Trans. Microwave Theory Tech., 1987, MTT-35, (12), pp.1288-1295

[5] CHANG, K.: Microwave ring circuits and antennas. New York: Wiley, 1996.

[6] HAMMERSTAD, E.O., and BEKKADAL, F.: *'A microstrip handbook,'* ELAB Report, STF44 A74169, N7034, University of Trondheim-NTH, NORWAY, 1975.